Brain Topography (2019) 32:1–16
https://doi.org/10.1007/s10548-018-0661-8

ORIGINAL PAPER

Robust Identification of Rich-Club Organization in Weighted and Dense Structural Connectomes

Xiaoyun Liang[1] · Chun-Hung Yeh[1] · Alan Connelly[1,2,3] · Fernando Calamante[1,2,3,4]

Received: 5 March 2018 / Accepted: 29 June 2018 / Published online: 3 July 2018

Abstract

The human brain is a complex network, in which some brain regions, denoted as 'hub' regions, play critically important roles. Some of these hubs are highly interconnected forming a rich-club organization, which has been identified based on the degree metric from structural connectomes constructed using diffusion tensor imaging (DTI)-based fiber tractography. However, given the limitations of DTI, the yielded structural connectomes are largely compromised, possibly affecting the characterization of rich-club organizations. Recent progress in diffusion MRI and fiber tractography now enable more reliable but also very dense structural connectomes to be achieved. However, while the existing rich-club analysis method is based on weighted networks, it is essentially built upon degree metric and, therefore, not suitable for identifying rich-club organizations from such dense networks, as it yields nodes with indistinguishably high degrees. Therefore, we propose a novel method, i.e. *R*ich-club organization *I*dentification using *C*ombined *H*-degree and *E*ffective strength to h-degree *R*atio (*RICHER*), to identify rich-club organizations from dense weighted networks. Overall, it is shown that more robust rich-club organizations can be achieved using our proposed framework (i.e., state-of-the-art fiber tractography approaches and our proposed RICHER method) in comparison to the previous method focusing on weighted networks based on degree, i.e., RC-degree. Furthermore, by simulating network attacks in 3 ways, i.e., attack to non-rich-club/non-rich-club edges (*NRC2NRC*), rich-club/non-rich-club edges (*RC2NRC*), and rich-club/rich-club edges (*RC2RC*), brain network damage consequences have been evaluated in terms of global efficiency (GE) reductions. As expected, significant GE reductions have been detected using our proposed framework among conditions, i.e., $NRC2NRC < RC2NRC$, $NRC2NRC < RC2RC$ and $RC2NRC < RC2RC$, which however have not been detected otherwise.

Keywords Rich club · *h-Degree* · Diffusion MRI · Fiber tractography · Structural connectome

Introduction

The human brain is a complex network, in which interacting brain regions (or nodes) are cooperative to perform complex function. Network analyses have shown that some highly connected and central brain regions, or so-called 'network hubs', play important roles in enabling efficient neuronal signaling and communication (Sporns et al. 2007). Furthermore, in healthy brains, some of these hub nodes have been

Xiaoyun Liang and Chun-Hung Yeh have contributed equally to this work.

Handling Editor: Fabrizio De Vico Fallani.

Electronic supplementary material The online version of this article (https://doi.org/10.1007/s10548-018-0661-8) contains supplementary material, which is available to authorized users.

✉ Xiaoyun Liang
imagetechliang@gmail.com

[1] The Florey Institute of Neuroscience and Mental Health, Heidelberg, VIC, Australia

[2] The Florey Department of Neuroscience and Mental Health Medicine, University of Melbourne, Melbourne, VIC, Australia

[3] Department of Medicine, Austin Health and Northern Health, University of Melbourne, Melbourne, VIC, Australia

[4] Present Address: Sydney Imaging and School of Aerospace, Mechanical and Mechatronic Engineering (Faculty of Engineering & Information Technologies), University of Sydney, Sydney, Australia

demonstrated to be more densely interconnected among themselves, together forming a core structure or 'rich-club' of the structural brain network (van den Heuvel and Sporns 2011; Colizza et al. 2006; Zhou and Mondragon 2004).[1] In this study, we investigate rich-club phenomenon based on this common description while other valid descriptions could be employed as well. Importantly, it has been shown that the disruption of the rich-club topology can be the underlying cause of global brain connectivity loss induced by brain diseases (van den Heuvel and Sporns 2011; van den Heuvel et al. 2013; McColgan et al. 2015).

The identification of rich-club architecture relies on the characteristics of the structural connectome. In the seminal study of brain rich-club organization (van den Heuvel and Sporns 2011), streamlines tractograms were reconstructed using diffusion tensor imaging (DTI) (Basser et al. 1994). This approach, however, is now recognized due to its failure to resolve fiber-crossing when tracking through areas with multiple fiber populations (Tournier et al. 2011). Furthermore, quantification of structural connectomes based on streamlines tractograms is known to be problematic (Jones et al. 2013). Issues related to the reconstruction of streamlines tractograms can be addressed using state-of-the-art techniques that have been specifically developed to correct for different sources of errors (Girard et al. 2014; Daducci et al. 2015; Smith et al. 2013; Pestilli et al. 2014). The application of these advanced techniques has been shown to improve the overall biologically plausibility and accuracy of connectome quantification (Smith et al. 2015). Furthermore, it has been demonstrated that these sources of tractogram biases/errors can alter the connectomic metrics significantly when using graph theory analysis (Yeh et al. 2016). Therefore, such tractogram bias/error corrections might also have major consequences in the characterization of rich-club organization.

Both the choice of tractogram algorithm (Bastiani et al. 2012) and brain parcellation (Zalesky et al. 2010) have been shown to have a major influence in the resulting network density for the structural connectome, e.g., from ~ 30% in van den Heuvel and Sporns (2011) to ~ 85% in Yeh et al. (2016), using the common atlas-based brain parcellation scheme (Desikan et al. 2006). Notably, some important network models, such as the small-world network architecture (Bullmore and Sporns 2012), are derived from the sparse network density of human brains. Accordingly, in order to conform with such inferences, sparse networks are commonly assumed in tractogram-based connectomic studies (Bullmore and Sporns 2009; Latora and Marchiori 2001, 2003). While arbitrary thresholding is usually applied to reduce network density through filtering out weak streamline connections, such processing has been demonstrated to cause detrimental effects on connectome characteristics (Drakesmith et al. 2015). To address this issue, a data driven approach was recently described to turn highly connected and weighted brain networks into sparse networks via thresholding, the method however requires the assumption that brain networks are sparse. Specifically, the underlying hypothesis of sparse structural network cannot be verified since a ground-truth fiber connectivity of the human brain currently does not exist. In fact, *dense* (66%) weighted structural networks have been confirmed in macaque cortical graphs using the retrograde tract tracing technique (Kennedy et al. 2013; Markov et al. 2011, 2013a). Given the high concordance between human and macaque brain systems shown in previous studies (Hutchison et al. 2012; Goulas et al. 2014), it is reasonable to infer that weighted structural networks of the human brain are also likely to be dense. Recently, Bassett and Bullmore 2016 advocated the use of weighted instead of binary networks, and they emphasized that such weighted and dense brain networks, including strong and weak connections, should provide a deeper and broader understanding of the brain network.

The key consequence of a highly-connected connectome is that one of the most fundamental network metrics, node *degree*, is no longer informative since most of the brain nodes have undistinguished high degrees (see Supplementary Fig. S1). More generally, such degree-based rich-club analysis could fail when degree parameter by which nodes are ranked provides limited resolution, regardless if networks are dense or sparse. Specifically, we focus on dense brain networks in this study. As a result, the computation of degree-related metrics or higher-order analyses need to be revisited (Yeh et al. 2016). Moreover, some important inferences limited to sparse network architecture might be no longer appropriate, such as the small-world network model, which was challenged by a recent study (Markov et al. 2013b). Likewise, the computation of the *weighted* rich-club coefficient (van den Heuvel and Sporns 2011), in which nodes are ranked using the *degree* metric, may not be appropriate for analyzing dense networks. *Degree* metric is likely to be more appropriate for binarized (i.e., *unweighted*) and sparse networks than for weighted and dense networks, which already unfavorably discards the important information of inter-areal weight heterogeneity (Markov et al. 2011).

When performing weighted analyses of structural connectomes, the node *strength*, typically defined as the number of streamlines directly linked to a node or the sum of inverse streamline lengths (Hagmann et al. 2008), is often used as edge weight (Barrat et al. 2004; Newman 2004; Opsahl et al. 2008). However, for any given network node, this

[1] Although rich-club formation could alternatively be present as a disassortative network, i.e., hubs tend to be more likely to be connected to low-degree nodes (Colizza et al. 2006), this is unlikely the case in the human brain network which has been proposed to be an assortative network (van den Heuvel and Sporns 2011) and therefore will not be considered in this study.

simple *strength* metric discards important information about the connection heterogeneity to the other relevant nodes. This issue can potentially be alleviated by the application of *h*-degree (Hirsch 2005) that has been shown to provide additional information in weighted network analyses (Zhao et al. 2011). The *h*-degree ranks a node by considering the connection strength between the relevant node pairs, which should therefore help to capture the weight heterogeneity that is fully neglected in the node *strength* metric. To help reader appreciate the issue of the application of traditional rich-club analysis approach to dense and weighted brain networks with different thresholds, traditional rich-club curves have been plotted without and with thresholds (see Supplementary Fig. S2).

In this study we extend the idea of *h*-degree and propose a novel method for identification of rich-club architecture from weighted connectomes (named RICHER, see "Methods" below), without making any assumptions on the brain network density. The performance of the proposed technique is evaluated with the following experiments: Firstly, we compare this new method with the commonly-used weighted rich-club analysis approach (van den Heuvel and Sporns 2011) for finding rich-club structures, by applying both approaches to the weighted connectomes generated from advanced tractogram reconstructions using anatomically-constrained tractography (ACT) (Smith et al. 2012) combined with spherical-deconvolution informed filtering of tractograms (SIFT) (Smith et al. 2013). Secondly, we compare the results with those derived from conventional DTI-based tractography, as employed by the pioneering work on rich-club architecture (van den Heuvel and Sporns 2011). Lastly, we perform permutation tests and simulations of network disruption to evaluate the significance and reliability of the resultant rich-club connectivity obtained from these methods of tractogram reconstructions and rich-club analyses.

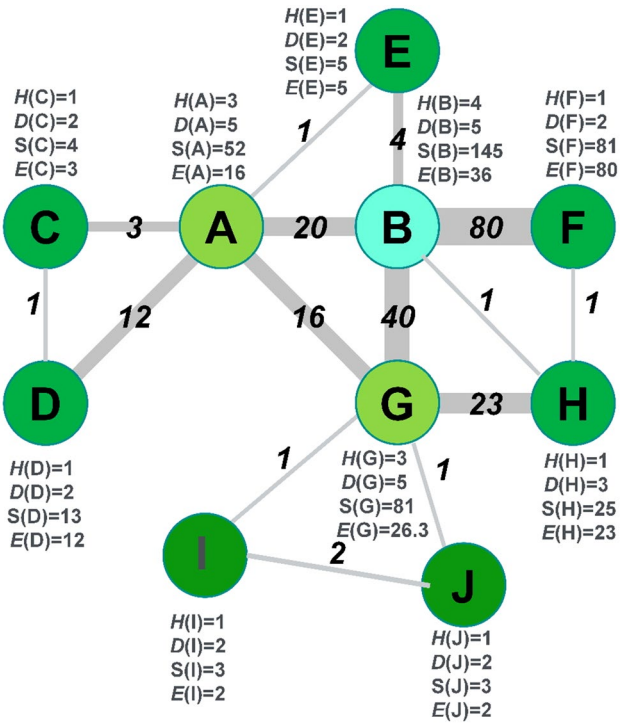

Fig. 1 Illustration of the relationships among network strength (*S*), h-degree (*H*) and effective strength to h-degree ratio (*E*). Each circle represents a node, and each line an edge (with strength given by the corresponding number); nodes with the same color have equal *h*-degree. Overall, node B is considered as the most important node among all 10 nodes, characterized by highest *H* and *E*. Furthermore, this example shows that while nodes F and G possess equivalent total strength (= 81), node G is characterized by a higher *h*-degree (i.e., $H = 3$ in comparisons to $H = 1$ for node F), demonstrating its more important role than that of strength; this suggests that *h*-degree is more capable of analyzing weighted networks. On the other hand, h-degree might not always be able to differentiate the importance of some nodes. For example, nodes A and G are both characterized by $H = 3$; however, node G is characterized by higher effective strength to *h*-degree ratio, i.e. $E(G) = 26.3$, than node A, $E(A) = 16$, indicating the more important role that node G might play in comparisons to A. Overall, nodes C, D, E, F, H, I & J are characterized by low *h*-degree (H = 1)

Materials and Methods

The Proposed Method: RICHER

We propose a novel method for identifying rich-club organization from weighted and dense structural networks, which is referred to as *R*ich-club organization *I*dentification using *C*ombined *H*-degree and *E*ffective strength to h-degree *R*atio (denoted as RICHER hereafter).

The Effective Strength to h-Degree Ratio

The network metric, *H-index (or h-degree)*, possesses advantages in analyzing weighted networks (Hirsch 2005; Zhao et al. 2011). The *h-degree H* of a node *i* in a weighted network is *H(i)* if *H(i)* is the largest number such that node *i* has at least *H* edges each with strength not less than *H(i)*.

In addition to *h-degree*, we introduce a complementary network metric, *effective strength to h-degree ratio, E*(*i*):

$$E(i) = S_{eff}(i)/H(i) \quad (1)$$

where $S_{eff}(i)$ is *effective strength* of node *i* (i.e. total connection strength of only the edges that contribute to *h-degree*), i.e., $E(i)$ corresponds to the average connection strength for the edges contributing to the *h-degree*.

This newly-defined metric can complement *h-degree* to distinguish between nodes with similar *h-degree* but different effective strength (see Fig. 1 for an illustrative example), with the underlying premise that a rich-club member

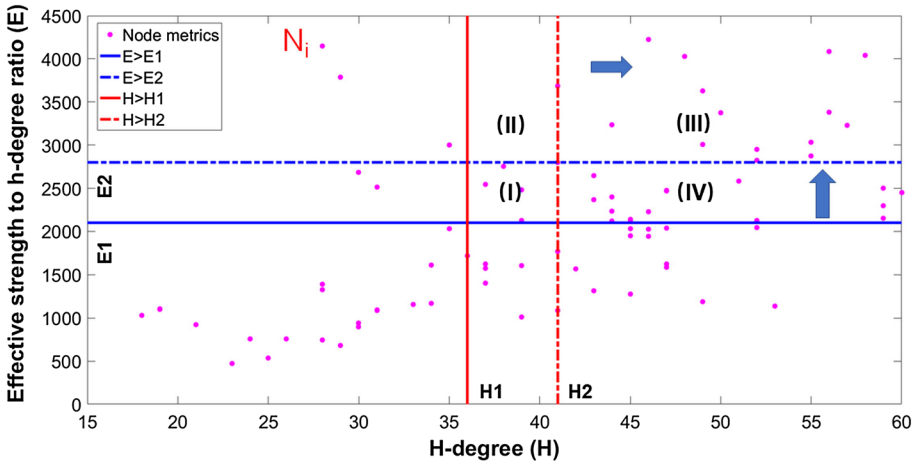

Fig. 2 Illustration of the proposed method, RICHER, for identifying rich-club organization. A searching region is continuously contracted if the current searching region does not constitute a rich-club organization, which is achieved by iteratively increasing thresholds for both h-degree (*H*) and effective strength to *h*-degree ratio (*E*). For simplicity's sake, only 2 instances (i.e., regions *R1* & *R2*) are exemplified. If a searching region *R1* is first selected as follows: $H \geq H1$ and $E \geq E1$ (including area I, II, III and IV encircled with solid black and blue lines); a subsequent contracted searching region *R2* is then selected as follows: $H \geq H2$ and $E \geq E2$ (including area III only encircled with dashed black and blue lines). The arrows demonstrate the contracted direction while running RICHER to identify rich-club organization

should fulfill two network characteristics (see Fig. 2): (1) high *H*, and (2) high *E*, i.e. a candidate rich-club should have *high h-degree* and *high strength per edge* at the same time. Note that the latter criterion should be strictly complied with the former, as brain regions merely having large *E* are not necessarily rich-club members. As illustrated in Fig. 1, for instance, '*node* H' is a segregated node that has relatively low *H* but with high *E* due to only one specific strong connections to its neighboring '*node* G'; since '*node* H' fails to satisfy the high *h-degree* criterion, it is not considered a rich-club member despite its high *E*.

Implementation

Criteria for Identifying Rich-Club Organization In practice, appropriate criteria are required to identify candidate nodes from a given (*H, E*) 'searching region' (i.e., an area confined by high *H* and *E* on a 2D graph, see Fig. 2). In previous studies, rich-club organization has been defined as a tendency for high-degree nodes to be more densely interconnected than nodes of a lower degree (van den Heuvel and Sporns 2011). Given that the degree metric is no longer appropriate for weighted and dense connectomes, the original strategy for identifying rich-club members is not applicable for RICHER. In this study, we therefore propose an analogous strategy for identifying rich-club nodes within a searching region: a rich-club member (i.e., *a node among those having both higher H and E*, as described in the previous section) must have stronger connections to the rich-club member set (*RC*) (i.e., total connection strength to potential rich-club organization divided by total number of potential rich-club members) than to the non-rich-club member set (*NRC*). This can be formulated as the following equation:

$$\forall n \in RC,\ R(n) = \frac{S_w(n)/N_{RC}}{S_b(n)/N_{NRC}} = \frac{\sum_{p \in RC} S_{n,p}/N_{RC}}{\sum_{q \in NRC} S_{n,q}/N_{NRC}} > 1 \quad (2)$$

where $S_w(n)$ is the sum of connection strengths between node *n* and other rich-club member *p* in *RC*, i.e., $S_{n,p}$; $S_b(n)$ is the sum of connection strengths between node *n* and other non-rich-club member *q* in *NRC*, i.e., $S_{n,q}$; $N_{RC}$and N_{NRC} are total number of members in *RC* and *NRC*, respectively. We consider that the ratio $R > 1$ is a necessary but non-sufficient condition that any *n* belonging to *RC* (i.e., within the 'searching region') must satisfy. Accordingly, we use this criterion to evaluate every candidate rich-club member within the searching region.

When the criterion of $R > 1$ is not fulfilled by all nodes in *RC*, we iteratively contract the 'searching region' (initialized by the area determined by $H > H1$ and $E > E1$; see Fig. 2, region I + II + III + IV, and next section for the choice of H1 and E1 values) by gradually increasing *E*; for each *E*, we then iteratively increase *H* and temporarily store every set of potential rich-club members that all satisfy the $R > 1$ condition. Essentially, this procedure is repeated across a range of *E* and *H* values and generates all potential sets of *RC*s. In order to determine the optimal *RC* across the predefined ranges of *E* and *H* values, i.e. among all potential sets of RCs, we propose choosing as the final rich-club organization the one that produces the largest Average Value of ratio *R*, denoted as

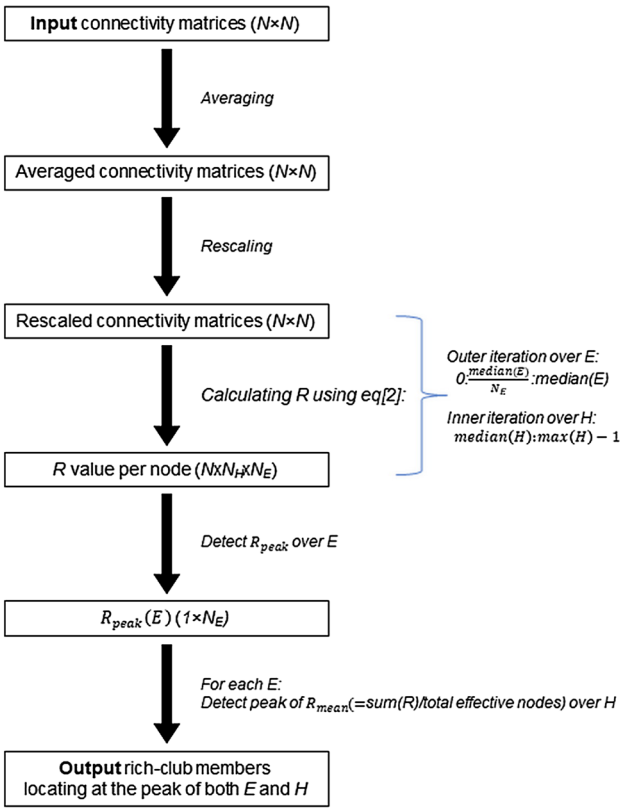

Fig. 3 The illustration of RICHER is shown in the flowchart. This flowchart should help reader understand RICHER better along with the pseudo code provided in the manuscript. Relevant parameters: *R* ratio coefficient, *H* h-degree, *E* H-degree ratio, N total number of brain regions, N_H total iteration steps of h-degree, N_E total iteration steps of E

AVR (AVR $= \frac{1}{N}\sum_{n\in RC} R(n)$, with *N* the total number of potential rich-club members). Note that we assign $AVR = 0$ if the $R > 1$ criterion is violated. The implementation of the RICHER approach is described with the following pseudo-code along with the flowchart (see Fig. 3):

In summary, the following criteria should be simultaneously satisfied for successfully extracting a rich-club organization.

1. The 'searching region' satisfies: $H1 \le H \le H_{max}$, and $E1 \le E \le E_{max}$;
2. $R > 1$ for every node within the searching region;
3. AVR of the preferred (final) rich-club organization should be equal to AVR_{max}, as computed above.

Defining a Range of Searching Regions The rich-club organization is formed only by a group of most important brain nodes (or so-called hubs), so it is reasonable to assume that the total number of rich-club members in the brain do not exceed half of the total nodes (Nigam et al. 2016; Crossley et al. 2013) while it might not be applicable to all network scenarios. Accordingly, the median value of *H* calculated from the connectome is selected as the starting values for *H1*, which is iterated until the maximum of *H*. We choose the range of *E* to lie between 0 and the median of *E*, i.e., *E1* = 0.

Addressing h-Degree Degradation to Degree Notably, one should be aware that *h-degree* might be unfavorably degraded to degree in certain situations. Taking an exceptional scenario as an example, when none of (or only a few of) the connection strengths are below the total number of nodes, the obtained *h-degree* metric is equivalent to the *degree* metric. To address this issue, we therefore propose the following approach to rescale the connectivity matrix to avoid *h-degree* degradation:

(1) Calculating median, minimum and maximum connection strength (S_{med}, S_{min} and S_{max}, respectively) across all connections;
(2) Applying linear rescaling mapping to all existing connections (i.e. with non-zero weight) with number of

For E = 0 : 1000 * 1 / 1000(median(E_0)), E_0 : E values of all nodes (We choose 1000 as the maximum number of iterations because E higher than its median value are excluded to avoid unfavorably discarding a subset of true rich-club members that have relatively high H but with E lower than their median values)

For H = median(H): maximum(H)-1

Compute $AVR(H,E) = \frac{1}{N}\sum_{n\in RC} R(n)$ ***(see Figure 2)***

End

Seek AVR_{max} ***(E) across H: the first peak of AVR(H, E)***

End

Seek AVR_{max} ***across E subject to AVRmax ≠ AVR(H, E=0)***

streamlines S less than S_{med}: $[S_{min}, S_{med}] \rightarrow [1, N/2]$, and calculating the scaling factor $SF = (N/2 - 1)/(S_{med} - S_{min})$, where N is the number of nodes in the parcellation (Note: N = 82 for the parcellation scheme used in our study);

(3) Each connection with S larger than S_{med} is then rescaled as follows: $S_{rescaled}(i,j) = (S(i,j) - S_{med}) * SF + N/2$, with i and j representing brain nodes. This rescaling approach aims to prevent *h-degree* from degrading to *degree*, thus ensuring the effectiveness of the RICHER method in identifying rich-club organizations from human brain structural connectomes.

To assess the suitability of the proposed rescaling approach, the original connections from the in vivo data included in this study were multiplied by a global scaling (approximately corresponding to a corresponding scaling to the value for the total number of streamlines used) to simulate the case of *h-degree* degradation. Furthermore, to incorporate the effect of noise, a small random per-edge scaling factor was also incorporated. Specifically, three simulated datasets were generated using three per-edge scaling factors obtained from a normal distribution with the mean (i.e., the global scaling factor) of 0.5, 4 or 10 and the standard deviation of 0.005, 0.04 or 0.1 respectively; these three scenarios are meant to simulate an analysis corresponding to half, 4 times and 10 times the total number of streamlines, respectively.

MRI Acquisition

Twenty-two healthy volunteers were recruited to participate in this study (females/males = 11/11; 32.5 ± 6.5 years old; all right-handed). All subjects provided written, informed consent, and all protocols were approved by the local Institutional Review Board. MRI data were acquired using a Siemens 3T Tim Trio system (Erlangen, Germany). Anatomical T1-weighted images were acquired using the three-dimensional magnetization-prepared rapid gradient echo sequence (MPRAGE) sequence (Mugler and Brookeman 1990) as follows: TR/TE/TI = 1900/2.6/900 ms, flip angle = 9°, field-of-view (FOV) = 230 × 230 mm^2, matrix size = 256 × 256, 192 sagittal slices, 0.9 mm isotropic resolution. Diffusion-weighted images (DWIs) were acquired using a twice-refocused spin-echo echo-planar imaging sequence (Reese et al. 2003) with the following parameters: TR/TE = 8400/110 ms, parallel imaging acceleration factor = 2, phase partial Fourier factor = 6/8, FOV = 240 × 240 mm^2, matrix size = 96 × 96, 60 axial slices at 2.5 mm isotropic voxel dimension, 60 diffusion sensitization directions with b = 3000 s/mm^2, and 8 b = 0 images. An additional pair of b = 0 images with reversed phase encoding polarity was acquired to enable correction of image distortion due to magnetic susceptibility effects.

Data Analysis

Data Pre-processing

DWIs were processed as follows: (1) Correction for susceptibility, eddy currents, and inter-volume motion artefacts using FSL's TOPUP and EDDY tools (Andersson et al. 2003; Smith et al. 2004); (2) Correction for B_1 bias field based on the mean $b = 0$ DWI using N4ITK (Tustison et al. 2010).

Anatomical T1 images were processed with the following steps: (1) Coregistration of T1 volumes to pre-processed mean $b = 0$ DWIs using SPM12 (http://www.fil.ion.ucl.ac.uk/spm/software/spm12/); (2) Estimation of tissue partial volume maps (PVMs) for brain WM, gray matter (GM), and CSF using FSL's segmentation tool (Smith et al. 2004); segmentation of subcortical GM using FSL's FIRST tool (Patenaude et al. 2011) in conjunction with a PVM estimation algorithm (Smith et al. 2012); merging all the PVMs together as required by ACT (Smith et al. 2012); (3) GM parcellation using the default FreeSurfer reconstruction pipeline (Dale et al. 1999) with 82 connectome nodes (i.e., excluding cerebellum) defined by the Desikan-Killiany cortical atlas segmentation (Desikan et al. 2006) (see Appendix for the complete list of labelled structural connectome nodes); replacing subcortical parcellations with estimates from FSL FLIRT (see Smith et al. 2015 for the full process of this step).

Tractogram Reconstruction

Fiber tracking was carried out using MRtrix (Tournier et al. 2012), with two different tracking strategies considered:

ACT + SIFT Fiber orientation distributions (FODs) were estimated using constrained spherical deconvolution (CSD) with a maximum spherical harmonic order of 8 (Tournier et al. 2007). Whole brain tractography was performed using the *2nd* order integration over fiber orientation distributions (iFOD2) probabilistic tracking algorithm (Tournier et al. 2010) combined with the ACT framework (Smith et al. 2012), using the following relevant parameters: step size = 1.25 mm, maximum curvature = 45° per step, streamlines length = 5–250 mm, FOD cutoff threshold = 0.1, and with the 'back-tracking' mechanism of the ACT framework. For each scan, tractograms of 10^8 streamlines were generated through seeding from WM mask. SIFT (Smith et al. 2013) was then applied to filter the reconstruction from 10^8 to 10^7 streamlines. Hereafter, this tracking strategy will be referred to as *advanced tractography* (**AT**).

Table 1 Eight results of rich-club organization investigated in this study: two methods, *RICHER* and *RC-degree*, were applied to the four connectomes, *ATSelAv, ATDirAv, DTSelAv* and *DTDirAv*, respectively

Connectomes	Methods	
	RC-degree	RICHER
ATSelAv	*ATSelAv* + RC-degree	*ATSelAv* + RICHER
ATDirAv	*ATDirAv* + RC-degree	*ATDirAv* + RICHER
DTSelAv	*DTSelAv* + RC-degree	*DTSelAv* + RICHER
DTDirAv	*DTDirAv* + RC-degree	*DTDirAv* + RICHER

DTI + FACT Conventional deterministic fiber-tracking was performed to generate 10^7 streamlines using the fiber assignment by continuous tracking (FACT) algorithm (Mori et al. 1999) with seeding from WM mask, step size = 0.25 mm, maximum curvature = 9° per step, length = 5–250 mm, fractional anisotropy cutoff = 0.1. Hereafter, this tracking strategy will be referred to as *DTI tractography* (**DT**); this tracking algorithm is also included in this study, for facilitating a more direct comparison to findings from the initial rich-club studies, which were based on this approach.

Connectome Construction

Individual-level connectomes were constructed by combining the streamline tractograms with subject GM parcellation. For AT, streamlines were assigned to the closest node within a 2-mm radius of the streamline endpoint (Smith et al. 2015). For DT, streamlines were assigned to the node at the voxels where track endpoints were located. To aggregate individual-level connectomes to group-level connectomes, two different ways were employed, following the methods described in van den Heuvel and Sporns (2011): (i) Direct Averaging (*DirAv*): The group-level connectome was obtained by averaging the connectomes across all subjects; (ii) Selective Averaging (*SelAv*): The group-level connectome was calculated by averaging those edges that were present in at least 75% of the subjects, i.e., all other entries were set to zero.

Therefore, four group-level connectomes were generated from two tractography (i.e. AT and DT) and two connectome averaging approaches (i.e., *SelAv* and *DirAv*). For convenience purposes, we used the abbreviations termed *ATSelAv, ATDirAv, DTSelAv*, and *DTDirAv* to denote these combinations in this article. Note that the purpose of employing *SelAv* and *DirAv* to generate group-level connectomes were twofold: (a) to assess if the identification of rich-club organization was affected by the way in which the group-level connectomes were aggregated; (b) to assess fault-tolerance of methods for identifying rich-club organization (see below).

Analyses of Rich-Club Characteristics

Identification of Rich-Club Organization For each group-level connectome, two methods were applied to identify the associated rich-club organization: (i) the traditional weighted rich-club analysis method based on degree metric (van den Heuvel and Sporns 2011), even though nodes are ranked based on strength, we use "*RC-degree*" to denote this technique, in order to differentiate it with h-degree employed in our proposed approach, and (ii) our proposed method, RICHER. Table 1 summarized the 8 conditions considered for rich-club analyses and comparisons in this study. For visualization purpose, rich-club brain regions are mapped onto Desikan-Killiany Atlas (Desikan et al. 2006) by using the BrainNet Viewer (http://www.nitrc.org/projects/bnv/).

Statistical Significance of Detected Rich-Club Organization To assess the statistical significance of the identified rich-club organization, permutation testing was employed (van den Heuvel and Sporns 2011). To achieve this goal, 1000 random networks were obtained by randomizing the network connections while keeping the degree distribution of sequence of the matrix unchanged (Rubinov and Sporns 2010). RICHER was then applied to identify potential rich-club organization from each of the randomized networks. The level of significance value, p, was computed by the fraction of rich-club detections, i.e., $p = n/1000$, where n is the total times of rich-club organization identified from the 1000 random networks. Thereby, $p < 0.05$ suggests that the identified rich-club organization was statistically significant.

Global Efficiency (GE) of Networks at Different 'Damage' Levels The rich-club regions have been shown to be critical for global communication of human brains (Harriger et al. 2012). The importance level of brain regions, such as the rich-club members, can be assessed by simulating network disruption caused by regional attacks with reduction in connection density among these regions. In this study, GE was employed to characterize the degree of network disruption following network attacks. Similar to the initial rich-club study (van den Heuvel and Sporns 2011), three different types of network attack were simulated: (i) Random attacks to connections within non-rich-club (NRC) regions, denoted as *NRC2NRC*; (ii) Random attacks to hub connections between rich-club (RC) and non-rich-club regions, denoted as *RC2NRC*; (iii) Targeted attacks to connections within rich-club regions, denoted as *RC2RC*.

Two network damage levels, the proportion τ (50 and 100%) of original weights, were simulated using Eq. (3) below:

$$W_{ij}^{\tau} = W_{ij}(1 - \tau/100). \quad (3)$$

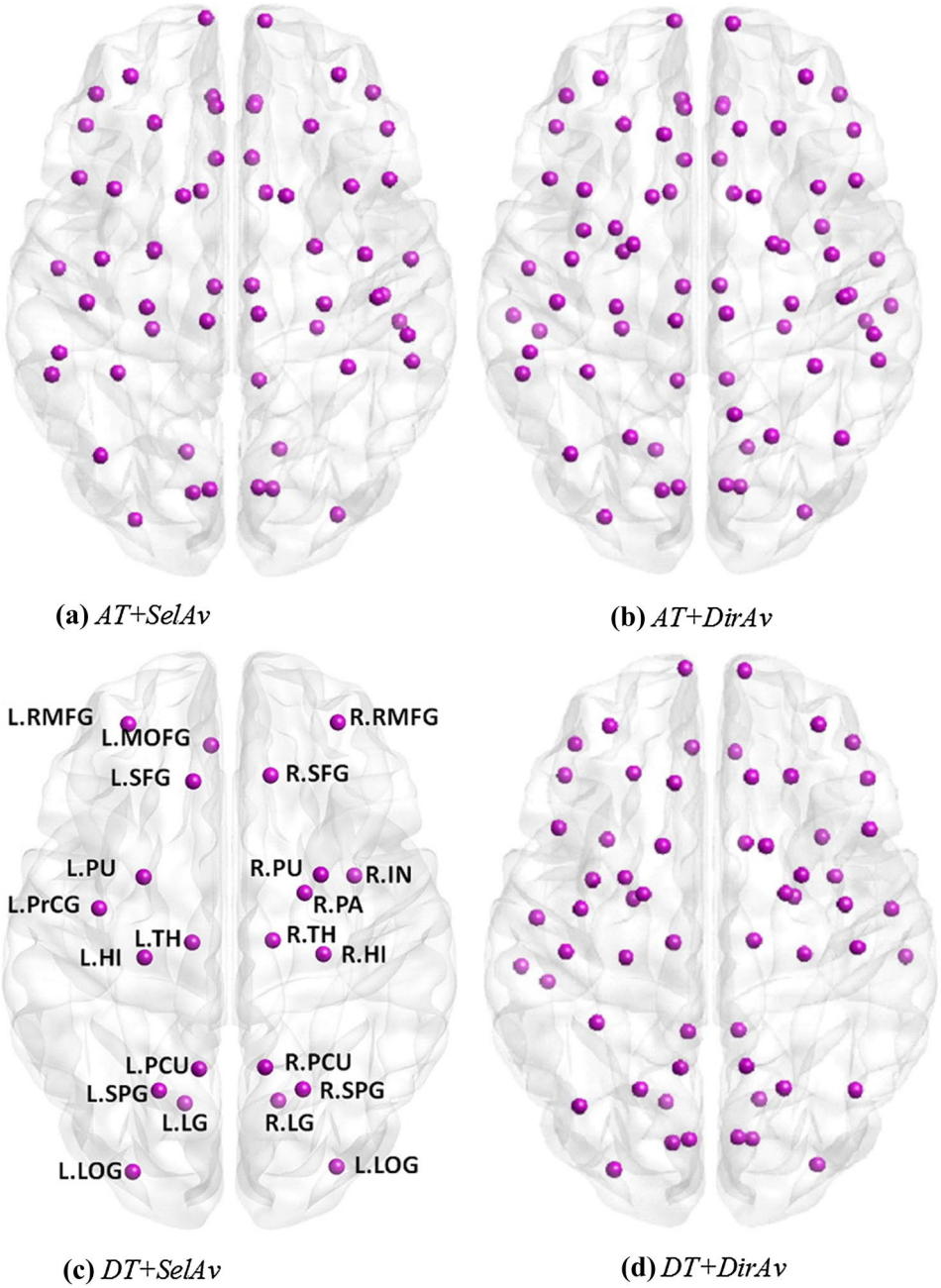

Fig. 4 Axial view of identified rich-club organization using the RC-degree method from the following four connectomes: **a** *ATSelAv*, **b** *ATDirAv*, **c** *DTSelAv* and **d** *DTDirAv. AT* advanced tractography, *DT* DTI tractography, *SelAv* selective averaging, *DirAv* direct averaging—see Sect. "Methods" for definitions. Due to the limited space, the names of structural labels are omitted for *ATSelAv, ATDirDV* and *DTDirAv*

W_{ij} and W_{ij}^{τ} indicated the edge intensity between nodes *i* and *j* before and after the network attack of damage level τ (van den Heuvel and Sporns 2011). Given the important role of rich-club members, it is therefore expected that *RC2RC* should have much stronger impact on GE than *NRC2NRC* and *RC2NRC* do. To evaluate the consequences of network attacks fairly, the total weight loss for *RC2RC, NRC2NRC* and *RC2NRC* should strictly match each other. Specifically, total loss of *RC2RC* is thus employed as a reference, while forcing total weight loss of *NRC2NRC* and *RC2NRC* to be equivalent to that of *RC2RC*. Note: Since this condition is however not always achievable due to excessively exaggerated number of rich-club members in some conditions, computing GEs for those cases where this condition is not met, therefore, were excluded from the study.

The statistical significance of GE reduction following three network attacks (i.e. *NRC2NRC, RC2NRC* and *RC2RC*) was evaluated using the following analyses (van den Heuvel and Sporns 2011). For each level of damage τ, 1000 random samples were generated for both *NRC2NRC* and *RC2NRC* by randomly attacking network edges while matching the total weight of damaged edges of both *NRC2NRC* and *RC2NRC*

Table 2 Number of rich-club members identified using RC-degree and RICHER from the following four connectomes: *ATSelAv, ATDirAv, DTSelAv* and *DTDirAv*

Connectomes	Network density (%)	Number of rich-club members identified using RC-degree	Number of rich-club members identified using RICHER
ATSelAv	81	61	19
ATDirAv	88	74	19
DTSelAv	36	22	22
DTDirAv	78	59	31

Results

Rich-Club Organization from the RC-Degree Method

Figure 4 shows rich-club organizations identified using the traditional RC-degree method. While only 22 rich-club members have been identified from *DTSelAv* (Fig. 4c), over half of the 82 brain regions have been unfavorably classified as rich-club members from networks obtained by using advanced tractography with both selective averaging (*ATSelAv*, Fig. 4a) and direct averaging (*ATDirAv*, Fig. 4b), and DTI tractography with direct averaging (*DTDirAv*, Fig. 3d), i.e., 61, 74 and 59, respectively; further inspections reveal that these three connectomes are overall characterized by much higher network density than

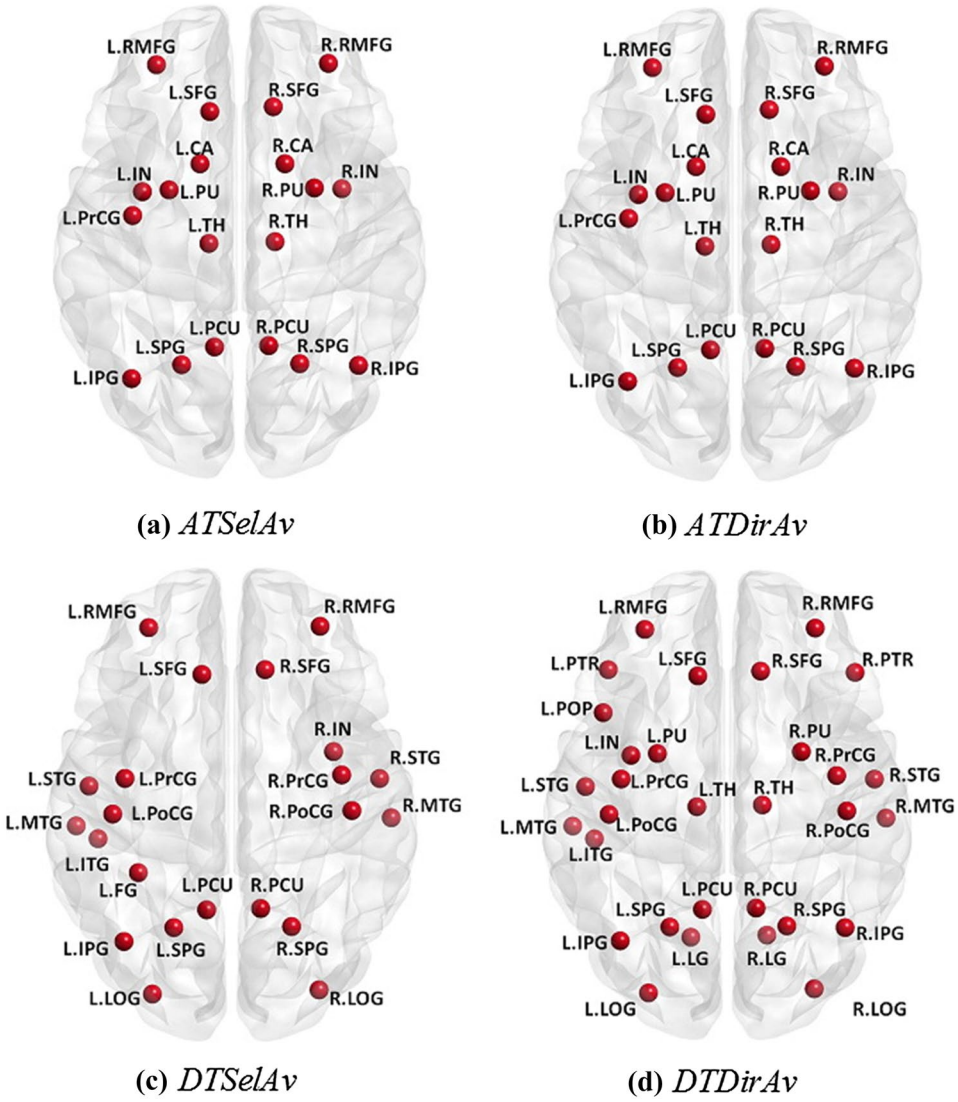

Fig. 5 Axial view of identified rich-club organization using the RICHER method from the following four connectomes: **a** *ATSelAv*, **b** *ATDirAv*, **c** *DTSelAv* and **d** *DTDirAv*. *AT* advanced tractography, *DT* DTI tractography, *SelAv* selective averaging *DirAv* direct averaging—Sect. "Methods" for definitions

to the reference value of *RC2RC*; otherwise, no random samples were generated. Permutation tests were then conducted to test statistical significance of *GE* decrease caused by the network attacks, i.e., *NRC2NRC, RC2NRC* and *RC2RC*.

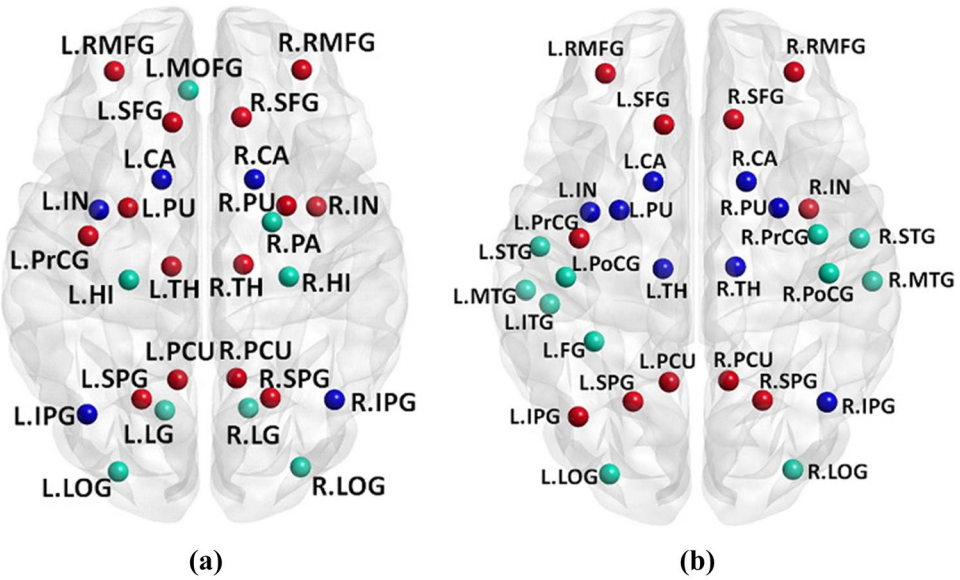

Fig. 6 Comparisons of identified rich-club organizations: **a** between conditions (I) *DTSelAv* + RC-degree and (II) *ATSelAv* + RICHER; **b** between conditions (III) *DTSelAv* + RICHER and (II) *ATSelAv* + RICHER. Nodes with red color represent rich-club members that are common for both conditions (i.e. **a** (I) and (II), **b** (III) and (II)), blue color represents rich-club members that are only present in: **a** (II) and **b** II, green color represents rich-club members that are only present in: **a** (I); and **b** III. *AT* advanced tractography, *DT* DTI tractography, *SelAv* selective averaging, *DirAv* direct averaging—see Sect. "Methods" for definitions

that of DTI tractography with selective averaging (*DTSelAv*) (see Table 2).

Rich-Club Organization from RICHER

Figure 5 shows the corresponding rich-club organizations identified using RICHER. In contrast to RC-degree, the number of rich-club members are much more consistent for all the four connectomes (see also Table 2). Notably, rich-club organizations identified from advanced tractography (i.e., *ATSelAv* and *ATDirAv*) using the RICHER method are exactly the same (see Fig. 5a, b), while rich-club organizations identified using the RICHER method from DTI tractography (i.e., *DTSelAv* vs. *DTDirAv*) are distinct (see Fig. 5c, d). Furthermore, permutation tests showed that these rich-club organization using RICHER are statistically significant with $p = 0$ (i.e., no rich-club organization was identified out of 1000 randomized networks).

Effect of Connectome Rescaling

Given the similarity between *ATSelAv* and *ATDirAv* results, the assessment of the rescaling approach for dealing with possible *h*-degree degradation (i.e. generating three simulated networks with different scaling factors) was done based on *ATSelAv*. Exactly the same rich-club members were obtained by applying the RICHER method to each of the three rescaled simulated networks (see Supplementary Fig. S3) in contrast to the obvious difference of identified rich-club members from simulated networks without rescaling, suggesting the proposed rescaling approach is able to avoid the h-degradation problem.

RC-Degree Versus RICHER and Effects of Tractography Methods

To further probe the differences in identifying rich-club organization between the proposed and the traditional approaches, the outcomes of the comparisons between (I) DTI tractography with selective averaging (*DTSelAv*) + RC-degree (Fig. 4c) and (II) advanced tractography with selective averaging (*ATSelAv*) + RICHER (Fig. 5a) are shown in Fig. 6a. Note that the result of *DTDirAv* + RC-degree is not considered for such comparisons since this approach does not provide a meaningful rich-club organization, as shown previously in Fig. 4d. Specifically, comparing to (I) *DTSelAv* + RC-degree, the following rich-club regions (labelled green in the figure) are *not* present in (II) *ATSelAv* + RICHER: *L.LOG, L.LG, L.MOFG, L.HI, R.PA, R.HI, R.LOG* and *R.LG*; the following rich-club regions (labeled blue) are *only* present in (II) *ATSelAv* + RICHER: *L.IPG, L.IN, L.CA, R.CA and R.IPG*. Figure 6a suggests that there are considerable differences between the conventional and the proposed framework to extract rich-club organizations.

To further segregate such differences that potential caused by tractography methods, the outcomes of the comparisons between (III) *DTSelAv* and (II) *ATSelAv* using RICHER (originated from Fig. 5a, c respectively) are shown in Fig. 6b. Comparing to the former, the latter does not have the following rich-club regions (green): *L.FG*, *L.ITG, L.LOG, L.MTG, L.PoCG, L.STG, R.LOG, R.MTG, R.PreCG, R.PoCG* and *R.STG;* the following ones (blue) are *only* present in the latter: *L.IN, L.CA, L.PU, L.TH, R.CA, R.IPG, R.PU* and *R.TH*. This reveals that the application of conventional or advanced tractography methods can have unneglectable effects on the computation of rich-club regions using RICHER.

Table 3 Global efficiencies (*GEs*) calculated from original networks and damaged networks attacked in three ways, i.e., *NRC2NRC, RC2NRC* and *RC2RC*, from eight conditions, i.e., *ATSelAv* + *RC-degree, ATDirAv* + RC-degree, *DTSelAv* + RC-degree, *DTDirAv* + RC-degree, *ATSelAv* + RICHER, *ATDirAv* + RICHER, *DTSelAv* + RICHER and *DTDirAv* + RICHER

Damage level (%)	Original GE	$GE_{NRC2NRC}$	GE_{RC2NRC}	GE_{RC2RC}
ATSelAv + RC-degree				
50	3728.7	NA	NA	NA
100	3728.7	NA	NA	NA
ATDirAv + RC-degree				
50	3728.7	NA	NA	NA
100	3728.7	NA	NA	NA
DTSelAv + RC-degree				
50	**1741.9**	**1583.9 + 31.1**	**1536.3 + 21.3**	**1544.4**
100	**1741.9**	**1525.9 + 47.4**	**1436.6 + 45.4**	**1437.3**
DTDirAv + RC-degree				
50	1741.9	NA	NA	NA
100	1741.9	NA	NA	NA
ATSelAv + RICHER				
50	**3728.7**	**3461.0 + 58.7**	**3355.3 + 36.9**	**3175.3**
100	**3728.7**	**3317.1 + 117.8**	**3184.5 + 62.1**	**2955.6**
ATDirAv + RICHER				
50	**3728.7**	**3457.9 + 67.7**	**3355.1 + 39.1**	**3175.3**
100	**3728.7**	**3318.3 + 71.4**	**3185.3 + 78.0**	**2955.6**
DTSelAv + RICHER				
50	**1741.9**	**1527.4 + 35.3**	**1406.6 + 17.7**	**1457.3**
100	**1741.9**	**1430.4 + 77.8**	**1300.8 + 51.2**	**1181.0**
DTDirAv + RICHER				
50	1741.9	NA	NA	NA
100	1741.9	NA	NA	NA

Rows with bold numbers were further plotted as bar graphs in Figs. 7 and 8

NA indicates that global efficiency (*GE*) cannot be calculated because total weight loss of damaged edges for either *NRC2NRC* or *RC2NRC* cannot match that of damaged edges to *RC2RC*

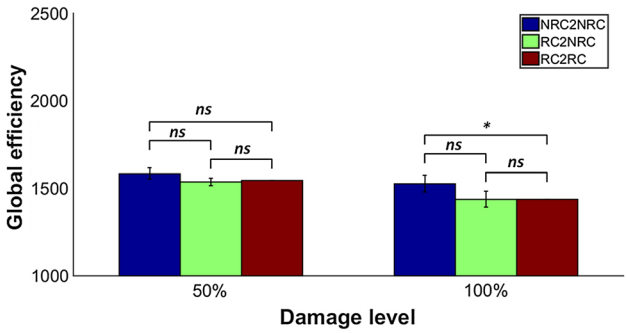

Fig. 7 Network attack targeted all connections among all identified rich-club members: Damage effects of three different ways, i.e., NRC2NRC, RC2NRC and RC2RC for *DTSelAv*, of which rich-club organization was identified using RC-degree at two damage levels (i.e., 50 and 100%). Permutation tests were employed to test whether comparisons of GE between the following conditions were significant or not: (i) *RC2RC* < NRC2NRC; (ii) RC2RC < RC2NRC, (iii) RC2NRC < NRC2NRC. *0.001 < p < 0.05; **p < 0.001; *ns* non-significant. *AT* advanced tractography, *DT* DTI tractography, *SelAv* selective averaging, *DirAv* direct averaging—see Sect. "Methods" for definitions

RC-Degree Versus RICHER Global Efficiency Reduction Following Network Attacks

The results of GE reduction following network damages (at two levels, $\tau = 50$ and 100%,) are summarized in Table 3; this corresponds to the scenario that network attack targeted all connections among all identified rich-club members (van den Heuvel and Sporns 2011). For each of the eight conditions (see Table 1), four average values of GE (among 1000 samples), i.e., GE_{ORIG}, $GE_{NRC2NRC}$, GE_{RC2NRC} and GE_{RC2RC}, are shown with standard deviations (ORIG: original network; NRC2NRC: Random attacks to connections within non-rich-club; RC2NRC: Random attacks to hub connections between rich-club and non-rich-club regions; RC2RC: Random attacks to connections within rich-club).

For a simpler representation of these results, Fig. 7 shows reductions in GEs under three attacking ways, *NRC2NRC, RC2NRC* and *RC2RC*, in *DTSelAv* + RC-degree (the combination traditionally most commonly used) at two damage levels, 50 and 100% (see Table 3 for more information about the other three conditions). Statistical analyses showed that significant differences are only present for $GE_{RC2RC} < GE_{NRC2NRC}$ at $\tau = 100\%$.

Figure 8 shows the corresponding results for RICHER in 3 conditions: *ATSelAv ATDirAv* and *DTSelAv*, at 2 damage levels, 50% and 100% (see Table 3 for more information about *DTDirAv* + RICHER). Specifically, the findings are as follows:

(i) Significant difference for each of the three comparisons, i.e., $GE_{RC2RC} < GE_{NRC2NRC}$, $GE_{RC2RC} < GE_{RC2NRC}$ and $GE_{RC2NRC} < GE_{NRC2NRC}$, has been favorably detected at $\tau = 50\%$ in both *ATSelAv* and *ATDirAv* using RICHER.
(ii) Significant differences have been detected for $GE_{RC2RC} < GE_{NRC2NRC}$ and $GE_{RC2RC} < GE_{RC2NRC}$ at $\tau = 100\%$ in both *ATSelAv* and *ATDirAv* using RICHER.
(iii) However, no significant difference has been detected for $GE_{RC2RC} < GE_{RC2NRC}$ at either damage level in *DTSelAv* using RICHER.

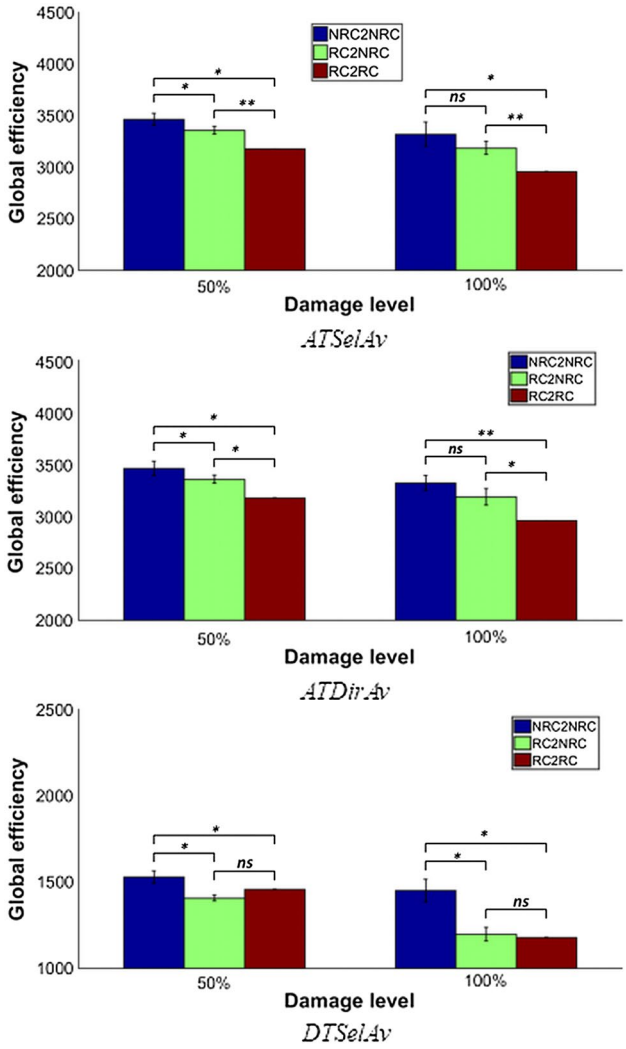

Fig. 8 Network attack targeted all connections among all identified rich-club members: Damage effects of three different ways, i.e., *NRC-2NRC, RC2NRC* and *RC2RC* for three conditions: *ATSelAv, ATDirAv* and *DTSelAv*, of which rich-club organization was identified using RICHER at two damage levels (i.e., 50 and 100%). Permutation tests were employed to test whether the following comparisons were significant or not: (i) *RC2RC* < *NRC2NRC;* (ii) *RC2RC* < *RC2NRC*; (iii) *RC2NRC* < *NRC2NRC*. *0.001 < p < 0.05; **p < 0.001; *ns* non-significant. *AT* advanced tractography, *DT* DTI tractography, *SelAv* selective averaging, *DirAv* direct averaging

Discussion

Robust identification of rich-club organization from structural networks plays an important role in further our understanding of network organization in the brain. In this study, *A*dvanced *T*ractography (*AT*, i.e. using CSD, ACT and SIFT), instead of *D*TI-based *T*ractography (*DT*), was employed to achieve more accurate estimation of structural connectomes (Smith et al. 2012, 2013), which in turn yielded weighted and dense networks. To tackle the problems of detecting rich-club organizations from such dense networks using the existing method, i.e. the traditional RC-degree method (van den Heuvel and Sporns 2011), a novel method, RICHER, relying on *h-degree*, has been proposed to robustly identify rich-club organizations. Our results highlight the necessity of applying new methods for robust definition of rich-club organization from weighted and dense networks; while RICHER was used here, it is by no means the only option, and other variants might be explored to achieve the same goal.

Rich-Club Mapping: Effects of Tractography and Rich-Club Identification Methods

Overall, by comparing among conditions, it has been shown in Figs. 4 and 5 that bilateral *RMFG, SFG, PCU, SPG,L. PrCG* and *R.IN* are identified as common rich-club members when using all approaches considered, indicating that these are more robust rich-club brain regions than others with respect to the methodology used to determine them. Specifically, five extra rich-club members (bilateral *CA, IPG and L.IN*), have been identified as rich-club members, characterized by relatively high *h*-degrees as well as high degrees (see Supplementary Table S1); however, these regions are unfavorably characterized by relatively low degrees from networks generated using *DTSelAv* (see Supplementary Table S1).

On the other hand, the bilateral *LOG* are identified as rich-club members from *DTSelAv*, irrespective of the rich-club computation method used, i.e., for both *DTSelAv* + RC-degree (Fig. 4c) and *DTSelAv* + RICHER (Fig. 5c), but are absence in *ATSelAv* + RICHER (Fig. 6b), suggests that disparities can also be caused by different tractography approaches used. Importantly, bilateral *HI, L.MOFG* and *R.PA* are only classified as rich-club members in *DTSelAv* + RC-degree (Fig. 4c), suggesting that, even if the network is sparse, identified rich-club organizations could still be largely affected by the method employed, i.e. RC-degree or RICHER. Notably, for those brain regions identified as rich-club members using the conventional *DTSelAv* + RC-degree, even though some of them have relatively high degree and/or h-degree, they are unfavorably characterized by relatively low effective strength to *h*-degree ratio (*E*) (i.e. bilateral *HI* and right *PA*; see Supplementary Table S1), thus discouraging them from being identified as rich-club members. This actually highlights the benefit of RICHER in which *h-degree* is used in conjunction with the metric *E* to effectively identify rich-club organization.

In summary, the abovementioned evidence indicates that identification of rich-club members is significantly affected not only by the rich-club computation algorithm (i.e. RC-degree and RICHER) but also by the tractography method (i.e., *AT* and *DT*).

Evidence Advocating the Use of Both AT and RICHER for Rich-Club Mapping

Our results have shown that the RC-degree method is *not* suitable for networks with high density, in which overestimation of rich-club organizations has been obtained from dense networks (see Table 2). In contrast, the RICHER method has more consistently identified reasonable number of rich-club members (e.g. number of rich-club members less than half of the total number of brain regions), whether the network density is high or low (see Table 2), suggesting that the RICHER method is more capable of identifying rich-club organizations from *both* sparse and dense networks.

Furthermore, identical rich-club members identified in *ATSelAv* and *ATDirAv* using RICHER (Fig. 5a, b) imply that the combination of advanced tractography and the RICHER method is robust to identifying rich-club organizations despite variations introduced by the averaging process. In contrast, rich-club members identified in *DT* using RICHER are quite different depending on the averaging method (*SelAv* vs. *DirAv*, shown in Fig. 5c, d), with associated number of rich-club members as follows: 22 versus 31, respectively. Overall, this is consistent with the outperformance of *AT* in comparison to *DT*. Importantly, these observed disparities in identified rich-club organizations collectively demonstrate that different fiber tracking approaches could lead to largely different rich-club organizations. Given the well-known limitations of DTI tractography (see Sect. "Introduction"), this advocates that more reliable fiber tracking techniques be employed to ensure that more robust networks are obtained for subsequent identification of rich-club organization. However, it should be noted that a robust identification of rich-club organization might only be achieved by combining robust fiber tracking approaches (such as *AT* in this study) and robust approaches for identifying rich-club organization (such as RICHER).

This is not the first study to avoid the limitation of DTI tractography when computing rich-club organizations. For example, CSD (Tournier et al. 2007) was recently employed to estimate the fiber orientation distribution, which was then used to investigate rich-club organizations (Wirsich et al. 2016; Roberts et al. 2016). Our study, however, also employed advanced tractography methods, such as ACT and SIFT, to correct tracking biases, so that more accurate structural connectomes can be achievable (Smith et al. 2015; Yeh et al. 2016). Of particular note, given that the *h-degree* based method, RICHER, is employed in our study, it is no longer restricted by the requirement that networks should be of relatively low (or medium) density, which might not be in fact the case. Practically, it has been shown in the current study that the network density of *DTDirAv* connectome could be very high (i.e., 78%), while network density of *DTSelAv* connectome is much lower (36%), due mainly to large inter-subject variability. In contrast, network densities of *ATSelAv* and *ATDirAv* connectomes are consistently high (i.e., 81 vs. 88%). Overall, this, therefore, strongly advocates the employment of the framework for combining *AT* and RICHER in robustly identifying rich-club organizations without being subject to the controversial restriction that the brain network is sparse (Kennedy et al. 2013; Markov et al. 2011, 2013a).

Simulated Attacks: Greatest GE Reductions Support the Proposed Framework

Furthermore, the validity of *ATSelAv* + RICHER and *ATDirAv* + RICHER in identifying rich-club organizations has been quantitatively demonstrated by statistically significant differences among simulated conditions (i.e., $GE_{RC2RC} < GE_{NRC2NRC}$, $GE_{RC2RC} < GE_{RC2NRC}$ at both damage levels (i.e., 50 and 100%), and $GE_{RC2NRC} < GE_{NRC2NRC}$ at $\tau = 50\%$) (see Fig. 8). In contrast, the absence of significant differences ($GE_{RC2RC} < GE_{RC2NRC}$, $GE_{RC2NRC} < GE_{NRC2NRC}$ at both damage levels, 50 and 100%, and $GE_{RC2RC} < GE_{NRC2NRC}$ at $\tau = 50\%$) using the RC-degree method (see Fig. 7) indicates that those identified rich-club members might not be as expected to have significantly stronger impact on GE of brain networks than the rest of the brain regions if they are disrupted, contradicting the expected key role rich-club members should play. Therefore, these results provide further quantitative evidence that identified rich-club organizations using the RC-degree method might not be reliable when used with dense weighted networks, while the proposed framework leads to more robust findings.

Brain Networks Not Necessarily Sparse

While previous rich-club studies have exclusively focused on sparse networks, it should be noted that these networks were either intentionally converted from dense networks by setting thresholds (McColgan et al. 2015), or constructed based on tractography methods known to have a number of limitations, such as DTI-based tractography (Tournier et al. 2011). In fact, weighted network density as high as 88% was found in our study and, as described in the Sect. "Introduction", high density can indeed occur in the brain (Kennedy et al. 2013; Markov et al. 2011, 2013a). Notably, while brain networks have been popularly considered to be sparse (Bullmore and Sporns 2009; Latora and Marchiori 2001, 2003), accumulating evidence has revealed that brain networks could be much denser than previously reported (Markov et al. 2013a, b; Yeh et al. 2016). Although obtained brain networks might be forced to be sparse by setting thresholds, this might, unfavorably,

alter the topology of the reconstructed brain networks with respect to the underlying true topology, therefore dramatically affecting the identification of rich-club organizations. Furthermore, the common approach to obtain sparse networks by removing relatively weak connections (i.e. those edges with strength below certain thresholds) has been challenged by the recent claim that weak connections are critically important in understanding neural systems (Bassett and Bullmore 2016).

Importantly, the proposed method, RICHER, avoids the need to constrain network density by somewhat arbitrarily setting connection strength thresholds. As such, by combining advanced tractography techniques with RICHER, it is reasonably expected that more accurate and robust identification of rich-club organizations can be favorably achieved, which might ultimately provide new insight into mechanisms underlying brain damage from a network point of view.

It should be noted that our study is conducted based on low-resolution region-based parcellations (Desikan et al. 2006). Intuitively, network density should decrease while increasing the resolution of brain parcellation (Zalesky et al. 2010). Therefore, one should be aware that, when discussing network density, it should be interpreted in the context of the specific brain parcellation employed. Nonetheless, as shown in our data, *RICHER* is capable of identifying rich-club organizations from either dense or sparse networks.

Limitations

In this study, our aim is to develop a viable rich-club analysis approach specifically for weighted and dense brain networks, as those obtained with more advanced fibre-tracking algorithms. We chose to compare our proposed method only with the outcomes obtained from the technique used in van den Heuval et al. (2011) based on the method proposed originally by Opsahl et al. (2008), since the latter is currently by far the most frequently-used approach to investigate the rich-club organization of the human brain. However, it would be interesting to perform systemic comparisons across a range of rich club computational techniques, which is beyond scope of the present manuscript.

In this study, our global connectome rescaling method attempts to empirically approximate the complex nonlinear problem to a more practically linear one, but this approach might not be an ideal solution. Nevertheless, as demonstrated by our simulated results (shown in the Supplementary Fig. S3), this rescaling approximation works well on mapping rich-club organization under a realistic range of experimental settings, suggesting that the proposed rescaling approach is a feasible practical solution for RICHER.

Recently, a weighted rich-club computation technique has been proposed, which enables generalization of various metrics into a single unified framework (Alstott et al. 2014). Although it might be beneficial to adapt RICHER to the definition formalized as in that study, the implementation is not likely to be simple. In practice, while implementing RICHER, the ratio R per node is computed iteratively for the detection of putative rich-club organizations, in order to find the greatest AVR to indicate the final outcome. Notably, since the underlying principle of RICHER is different, how feasible the relevant parameters could potentially be expressed by the metrics defined within the unified framework remains a topic of further investigation; this however is beyond the scope of the present study.

Conclusion

In this study, we have employed a sophisticated fiber tractography method, i.e., CSD-based calculation of fiber orientation followed by tracking biases correction strategies using ACT and SIFT, to ensure more accurate estimation of structural connectomes, yielding weighted and very dense networks. Importantly, it has also been demonstrated that the traditional method, RC-degree, is incapable of identifying rich-club organizations from such dense networks. Therefore, a novel method, RICHER, has been proposed to address this issue. Our results have shown that RICHER is capable of identifying rich-club organizations from not only sparse but also very dense networks, which has been further corroborated by the evidence that greatest global efficiency reductions have been caused by simulated damages in rich-club organizations identified using RICHER among all simulations. Overall, our study has demonstrated that upon application of state-of-the-art fiber tractography methods and the RICHER method, robust rich-club organizations can be reliably identified from diffusion MRI data without having to rely on a binary approach or an arbitrary threshold strategy to impose low density. This might, therefore, be more beneficial for future brain connectome research that focuses on identifying dysfunctional rich-club members from cohorts with brain disorders.

Acknowledgements We thank Dr. Robert Elton Smith (Florey Institute of Neuroscience and Mental Health) for very helpful discussions and advice. We are grateful to the National Health and Medical Research Council (NHMRC) of Australia, the Australian Research Council (ARC), and the Victorian Government's Operational Infrastructure Support Program for their support. The authors also acknowledge the facilities, and the scientific and technical assistance of the National Imaging Facility at the Florey Node.

Funding Funding was provided by National Health and Medical Research Council (Grant Nos. 1091593 and APP1117724).

References

Alstott J, Panzarasa P, Rubinov M, Bullmore ET, Vertes PE (2014) A unifying framework for measuring weighted rich clubs. Sci Rep 4:7258

Andersson JL, Skare S, Ashburner J (2003) How to correct susceptibility distortions in spin-echo echo-planar images: application to diffusion tensor imaging. Neuroimage 20:870–888

Barrat A, Barthelemy M, Pastor-Satorras R, Vespignani A (2004) The architecture of complex weighted networks. Proc Natl Acad Sci USA 101:3747–3752

Basser PJ, Mattiello J, Lebihan D (1994) Estimation of the effective self-diffusion tensor from the NMR spin echo. J Magn Reson B 103:247–254

Bassett DS, Bullmore ET (2016) Small-world brain networks revisited. Neuroscientist 23:499–516

Bastiani M, Shah NJ, Goebel R, Roebroeck A (2012) Human cortical connectome reconstruction from diffusion weighted MRI: the effect of tractography algorithm. Neuroimage 62:1732–1749

Bullmore E, Sporns O (2009) Complex brain networks: graph theoretical analysis of structural and functional systems. Nat Rev Neurosci 10:186–198

Bullmore E, Sporns O (2012) The economy of brain network organization. Nat Rev Neurosci 13:336–349

Colizza V, Flammini A, Serrano MA, Vespignani A (2006) Detecting rich-club ordering in complex networks. Nat Phys 2:110–115

Crossley NA, Mechelli A, Vertes PE, Winton-Brown TT, Patel AX, Ginestet CE, Mcguire P, Bullmore ET (2013) Cognitive relevance of the community structure of the human brain functional coactivation network. Proc Natl Acad Sci USA 110:11583–11588

Daducci A, Dal Palu A, Lemkaddem A, Thiran JP (2015) COMMIT: Convex optimization modeling for microstructure informed tractography. IEEE Trans Med Imaging 34:246–257

Dale AM, Fischl B, Sereno MI (1999) Cortical surface-based analysis. I. Segmentation and surface reconstruction. Neuroimage 9:179–194

Desikan RS, Segonne F, Fischl B, Quinn BT, Dickerson BC, Blacker D, Buckner RL, Dale AM, Maguire RP, Hyman BT, Albert MS, Killiany RJ (2006) An automated labeling system for subdividing the human cerebral cortex on MRI scans into gyral based regions of interest. Neuroimage 31:968–980

Drakesmith M, Caeyenberghs K, Dutt A, Lewis G, David AS, Jones DK (2015) Overcoming the effects of false positives and threshold bias in graph theoretical analyses of neuroimaging data. Neuroimage 118:313–333

Girard G, Whittingstall K, Deriche R, Descoteaux M (2014) Towards quantitative connectivity analysis: reducing tractography biases. Neuroimage 98:266–278

Goulas A, Bastiani M, Bezgin G, Uylings HB, Roebroeck A, Stiers P (2014) Comparative analysis of the macroscale structural connectivity in the macaque and human brain. PLoS Comput Biol 10:e1003529

Hagmann P, Cammoun L, Gigandet X, Meuli R, Honey CJ, Wedeen VJ, Sporns O (2008) Mapping the structural core of human cerebral cortex. PLoS Biol 6:e159

Harriger L, Van Den Heuvel MP, Sporns O (2012) Rich club organization of macaque cerebral cortex and its role in network communication. PLoS ONE 7:e46497

Hirsch JE (2005) An index to quantify an individual's scientific research output. Proc Natl Acad Sci USA 102:16569–16572

Hutchison RM, Gallivan JP, Culham JC, Gati JS, Menon RS, Everling S (2012) Functional connectivity of the frontal eye fields in humans and macaque monkeys investigated with resting-state fMRI. J Neurophysiol 107:2463–2474

Jones DK, Knosche TR, Turner R (2013) White matter integrity, fiber count, and other fallacies: the do's and don'ts of diffusion MRI. Neuroimage 73:239–254

Kennedy H, Knoblauch K, Toroczkai Z (2013) Why data coherence and quality is critical for understanding interareal cortical networks. Neuroimage 80:37–45

Latora V, Marchiori M (2001) Efficient behavior of small-world networks. Phys Rev Lett 87:198701

Latora V, Marchiori M (2003) Economic small-world behavior in weighted networks. Eur Phys J B 32:249–263

Markov NT, Misery P, Falchier A, Lamy C, Vezoli J, Quilodran R, Gariel MA, Giroud P, Ercsey-Ravasz M, Pilaz LJ, Huissoud C, Barone P, Dehay C, Toroczkai Z, Essen V, Kennedy DC, Knoblauch K (2011) Weight consistency specifies regularities of macaque cortical networks. Cereb Cortex 21:1254–1272

Markov NT, Ercsey-Ravasz M, Lamy C, Ribeiro Gomes AR, Magrou L, Misery P, Giroud P, Barone P, Dehay C, Toroczkai Z, Knoblauch K, Van Essen DC, Kennedy H (2013a) The role of long-range connections on the specificity of the macaque interareal cortical network. Proc Natl Acad Sci USA 110:5187–5192

Markov NT, Ercsey-Ravasz M, Van Essen DC, Knoblauch K, Toroczkai Z, Kennedy H (2013b) Cortical high-density counterstream architectures. Science 342:1238406

Mccolgan P, Seunarine KK, Raz i A, Cole JH, Gregory S, Durr A, Roos RA, Stout JC, Landwehrmeyer B, Scahill RI, Clark CA, Rees G, Tabrizi SJ, Track HD I (2015) Selective vulnerability of Rich Club brain regions is an organizational principle of structural connectivity loss in Huntington's disease. Brain 138:3327–3344

Mori S, Crain BJ, Chacko VP, Van Zijl PC (1999) Three-dimensional tracking of axonal projections in the brain by magnetic resonance imaging. Ann Neurol 45:265–269

Mugler JP, 3RD and Brookeman JR (1990) Three-dimensional magnetization-prepared rapid gradient-echo imaging (3D MP RAGE). Magn Reson Med 15:152–157

Newman MEJ (2004) Analysis of weighted networks. Phys Rev E 70:056131

Nigam S, Shimono M, Ito S, Yeh FC, Timme N, Myroshnychenko M, Lapish CC, Tosi Z, Hottowy P, Smith WC, Masmanidis SC, Litke AM, Sporns O, Beggs JM (2016) Rich-club organization in effective connectivity among cortical neurons. J Neurosci 36:670–684

Opsahl T, Colizza V, Panzarasa P, Ramasco JJ (2008) Prominence and control: the weighted rich-club effect. Phys Rev Lett, 101:168702

Patenaude B, Smith SM, Kennedy DN, Jenkinson M (2011) A Bayesian model of shape and appearance for subcortical brain segmentation. Neuroimage 56:907–922

Pestilli F, Yeatman JD, Rokem A, Kay KN, Wandell BA (2014) Evaluation and statistical inference for human connectomes. Nat Methods 11:1058–1063

Reese TG, Heid O, Weisskoff RM, Wedeen VJ (2003) Reduction of eddy-current-induced distortion in diffusion MRI using a twice-refocused spin echo. Magn Reson Med 49:177–182

Roberts JA, Perry A, Lord AR, Roberts G, Mitchell PB, Smith RE, Calamante F, Breakspear M (2016) The contribution of geometry to the human connectome. Neuroimage 124:379–393

Rubinov M, Sporns O (2010) Complex network measures of brain connectivity: uses and interpretations. Neuroimage 52:1059–1069

Smith SM, Jenkinson M, Woolrich MW, Beckmann CF, Behrens TE, Johansen-Berg H, Bannister PR, De Luca M, Drobnjak I, Flitney DE, Niazy RK, Saunders J, Vickers J, De Stefano Zhang Y, Brady N, Matthews PM (2004) Advances in functional and structural MR image analysis and implementation as FSL. Neuroimage 23 Suppl 1, S208-19

Smith RE, Tournier JD, Calamante F, Connelly A (2012) Anatomically-constrained tractography: improved diffusion MRI streamlines

tractography through effective use of anatomical information. Neuroimage 62:1924–1938
Smith RE, Tournier JD, Calamante F, Connelly A (2013) SIFT: Spherical-deconvolution informed filtering of tractograms. Neuroimage 67:298–312
Smith RE, Tournier JD, Calamante F, Connelly A (2015) The effects of SIFT on the reproducibility and biological accuracy of the structural connectome. Neuroimage 104:253–265
Sporns O, Honey CJ, Kotter R (2007) Identification and classification of hubs in brain networks. PLoS ONE 2:e1049
Tournier JD, Calamante F, Connelly A (2007) Robust determination of the fibre orientation distribution in diffusion MRI: non-negativity constrained super-resolved spherical deconvolution. Neuroimage 35:1459–1472
Tournier JD, Calamante F, Connelly A (2010) Improved probabilistic streamlines tractography by 2nd order integration over fibre orientation distributions. Proc ISMRM 18:1670
Tournier JD, Mori S, Leemans A (2011) Diffusion tensor imaging and beyond. Magn Reson Med 65:1532–1556
Tournier JD, Calamante F, Connelly A (2012) MRtrix: Diffusion tractography in crossing fiber regions. Int J Imaging Syst Technol 22:53–66
Tustison NJ, Avants BB, Cook PA, Zheng Y, Egan A, Yushkevich PA, Gee JC (2010) N4ITK: improved N3 bias correction. IEEE Trans Med Imaging 29:1310–1320
Van Den Heuvel MP, Sporns O (2011) Rich-club organization of the human connectome. J Neurosci 31:15775–15786
Van Den Heuvel MP, Sporns O, Collin G, Scheewe T, Mandl RC, Cahn W, Goni J, Pol H, Kahn RS (2013) Abnormal rich club organization and functional brain dynamics in schizophrenia. JAMA Psychiatry 70:783–792
Wirsich J, Perry A, Ridley B, Proix T, Golos M, Benar C, Ranjeva J-P, Bartolomei F, Breakspear M, Jirsa V, Guye M (2016) Whole-brain analytic measures of network communication reveal increased structure-function correlation in right temporal lobe epilepsy. Neuroimage https://doi.org/10.1016/j.nicl.2016.05.010
Yeh CH, Smith RE, Liang X, Calamante F, Connelly A (2016) Correction for diffusion MRI fibre tracking biases: The consequences for structural connectomic metrics. Neuroimage https://doi.org/10.1016/j.neuroimage.2016.05.047
Zalesky A, Fornito A, Harding IH, Cocchi L, Yucel M, Pantelis C, Bullmore ET (2010) Whole-brain anatomical networks: does the choice of nodes matter? Neuroimage 50:970–983
Zhao SX, Rousseau R, Ye FY (2011) h-Degree as a basic measure in weighted networks. J Inform 5:668–677
Zhou S, Mondragon RJ (2004) The rich-club phenomenon in the Internet topology. IEEE Commun Lett 8:180–182